

DAFS Experiments with Non-Centrosymmetric Single Crystals

Dirk C. Meyer,^a Kurt Richter,^a Andreas Seidel,^a Jörg Weigelt,^b Ronald Frahm^b and Peter Paufler^{a*}

^aInstitut für Kristallographie und Festkörperphysik, Fachrichtung Physik der TU, D-01062 Dresden, Germany, and ^bHamburger Synchrotronstrahlungslabor HASYLAB at DESY, D-22603 Hamburg, Germany. E-mail: paufler@physik.tu-dresden.de

(Received 24 July 1997; accepted 11 March 1998)

Diffraction anomalous fine structure (DAFS) experiments were applied to an epitaxially grown (Ga,In)P layer on a [001] GaAs substrate as a single-crystalline model substance. The requirements for the reliable measurement of reflection intensities as a function of photon energy, as well as the quantitative DAFS analysis resulting in the complex-valued fine-structure function of the scattering factor, are described. In the case of single crystals, effort had to be put into performing the DAFS measurements in order to hold the position of the Bragg reflection exactly during the energy scan. Using the zinc-blende-type structure as an example, it is shown for the first time that, similar to single-crystal structure analysis, the lack of inversion symmetry has a significant impact on the DAFS signal, so that DAFS may contribute to structure analysis as well.

Keywords: DAFS; (Ga,In)P; structure factors; non-centrosymmetric crystals.

1. Introduction

Synchrotron radiation enables a continuous variation of the wavelength of the incident beam of value $\Delta\lambda$. When $\Delta\lambda$ spans the absorption edge of one of the atomic species involved in the standing-wave field of Bragg reflection, an oscillation of the Bragg intensity occurs analogous to that of X-ray absorption fine structure (XAFS). Since the intensity, I , of X-ray diffraction (XRD) is proportional to the square of the atomic scattering factor, which in turn contains the anomalous dispersion term $\Delta f = f' + if''$, f'' being proportional to the absorption cross section, absorption-like information can be expected from precise measurements of I . Considering that the physical process behind this oscillation is the same as for XAFS, the phenomenon has been called 'Bragg reflectivity extended fine structure' (BREFS) by Arcon *et al.* (1987) and later on 'diffraction anomalous fine structure' (DAFS) by Stragier *et al.* (1992). In fact, as will be shown below, DAFS can provide the same information about the local structure of resonant atoms as XAFS does.

Moreover, the combined technique is not just the simultaneous performance of an XAFS and an XRD experiment but the intersection of both. That is, only those atoms which contribute to the Bragg reflection under consideration have an impact on the DAFS signal. DAFS enables the selection of (even a small) part of the specimen for short-range-order analysis. This part might differ in orientation, lattice parameters or structure from the rest of the specimen. If XAFS is measured simultaneously, this signal will arise from all resonating atoms throughout the sample (Fig. 1).

This means two enhanced sensitivities (wavevector and energy) of DAFS experiments instead of one (energy) with XAFS measurements. The XAFS signal is an average over the whole sample.

Arcon *et al.* (1987), Stragier *et al.* (1992), Sorensen *et al.* (1994) and Mizuki (1996) have surveyed DAFS history, theory, experimental methods, data analysis techniques and some applications in detail. The reader is referred to these publications for further study. Rather stringent experimental requirements are the single-crystal monochromator for energy variation and, in the case of angle-dispersive diffraction, the goniometer to preserve the Bragg angle of reflection during the energy scan. We have outlined the possibility of DAFS experiments using polychromatic synchrotron radiation and a single crystal acting as the specimen as well as the monochromator (Meyer *et al.*, 1994).

Arndt *et al.* (1982) used the polychromatic synchrotron radiation beam in connection with a suitably curved crystal monochromator to establish an energy/angular-dispersive diffraction set-up. Every reflection in the diffraction pattern can then contain a complete energy profile across the absorption edge of one of the atoms. By comparing the reflections free of an anomalous scatterer contribution with the reflections influenced by resonant atoms, an absorption correction can be applied. Using the same idea and a two-dimensional detector, Lee *et al.* (1994) have drawn attention to the possibility of time-resolved DAFS while Hodeau *et al.* (1995) have obtained results comparable with DAFS measurements of both modes, the energy/angular-dispersive mode and the mode with a double-crystal monochromator. They succeeded, for example, in the

determination of the Fe cation tetrahedral and octahedral site contributions to the anomalous scattering factor in hexagonal ferrite BaZnFeO_{11} . Renevier *et al.* (1995) studied the local structure of Ir layers in Ir(100)/Fe superlattices by DAFS at the Ir L_3 -edge. Ravel *et al.* (1995) applied typical XAFS computer programs to handle DAFS spectra. Vacinova *et al.* (1995) described DAFS measurements of small single crystals of barium platinum oxide.

The aim of the present communication is to demonstrate the application of DAFS to a single crystalline thin film of a non-centrosymmetric structure. The system studied was a (Ga,In)P monolayer (layer thickness $1.9 \mu\text{m}$) grown on a (001) GaAs substrate. The solid solution (Ga,In)P is subject to ordering on particular planes (Ueda *et al.*, 1987), a challenge for selective short-range-order analysis. Our results on the ordering phenomenon itself are dealt with elsewhere (Meyer *et al.*, 1998).

2. Experimental

Our DAFS experiments were carried out at the undulator beamline BW1 of the Hamburg synchrotron radiation laboratory using an Si(111) double-crystal monochromator. The set-up is shown in Fig. 2. An eight-circle diffractometer available at this measuring station was supplemented with a piezoelectric tilting table. Both reflection intensity and Ga

K -fluorescence intensity were recorded simultaneously using thermoelectrically cooled Si PIN photodiodes (Meyer *et al.*, 1995) in the current mode.

The incoming monochromatic beam (photon energies near the Ga K -edge at about 10367 eV) was limited by slits ($0.7 \text{ mm} \times 2.62 \text{ mm}$) and monitored by an ionization chamber situated between the slits and specimen. A 0.4 mm slit in front of the reflection detector reduced the fluorescence background and prohibited the simultaneous detection of the closely adjacent substrate reflection. To obtain a sufficiently high angular resolution for the separation of substrate and layer reflections, we have chosen the (Ga,In)P 333 and $\bar{3}\bar{3}3$ reflections for our DAFS experiments. The polarization vector of the radiation was parallel to the normal of the scattering plane.

Preliminary Bragg-angle adjustment of the specimen was performed using the sample goniometer (θ rotation, Ψ tilt angle). $\theta(E)$ was programmed according to a second-order polynomial which had been worked out beforehand with the aid of a diffraction pre-experiment. Because of the narrow single-crystal reflection, the accuracy of the θ -setting ($\Delta\theta = 0.001^\circ$) by the sample goniometer was insufficient for preserving the Bragg peak when changing the photon energy E . For DAFS measurements with perfect single crystals an accuracy in θ -positioning of about 0.0001° is necessary. We achieved this by adding a special sample

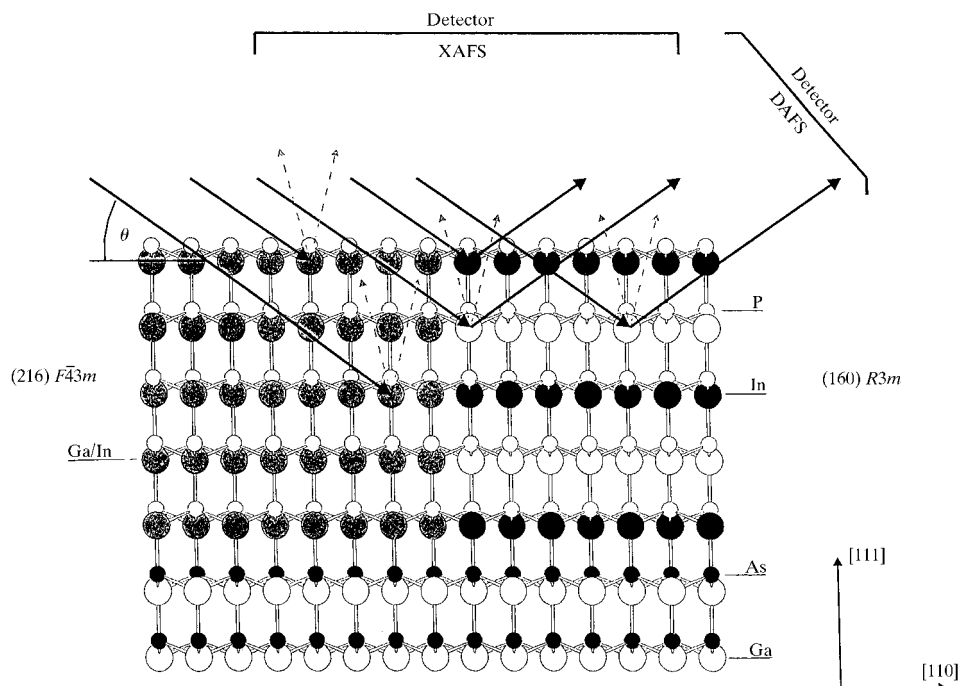


Figure 1

Diagram to illustrate the difference between XAFS and DAFS. When an incident X-ray beam with energy slightly above the absorption edge of Ga hits Ga atoms (statistically distributed among grey circles on the left and placed on white circles on the right) at Bragg angle θ , characteristic Ga K radiation from atoms all over the specimen will be collected using the XAFS detector. The DAFS detector, however, will see a Bragg reflection intensity from the ordered part of the specimen only (right), which in turn is influenced solely by those resonant atoms which contribute to the Bragg reflection. Using a superlattice reflection of rhombohedrally ordered (Ga,In)P, DAFS thus probes the short-range order of a subset of Ga atoms instead of averaging all Ga atoms.

holder [adapted to the flat specimen; surface almost parallel to the (001) planes of (Ga,In)P and GaAs] together with a piezoelectric translator used as a tilting table (Physik Instrumente GmbH, type P-287.70).

The basic idea for the fine adjustment of the specimen is to overcome the difficulty of exactly setting the Bragg angle using a dynamic positioner. This was achieved by a special control set-up supplying the scanning high voltage for the piezoelectric element which enabled the specimen to be tilted symmetrically with respect to the Bragg angle. This proved time-saving compared with a step-by-step rocking of the specimen at every energy step, although a delay time of several seconds is necessary to hit the corrected angle at every energy step.

The control set-up for the high-voltage supply consisted of a lock-in amplifier with reference oscillator (ITHACO Dynatrac, model 393) and a high-voltage operational amplifier (Physik Instrumente GmbH, Modul E-107). The high-voltage operational amplifier provided a d.c. voltage (0–1000 V) that sets the mean angle of the specimen and a small modulation signal that results in an a.c. component in the reflected X-ray signal. The photocurrent of the PIN photodiode detecting the reflected X-rays was amplified by a fast current amplifier (Keithley Instruments, model 428). The output signal of the current amplifier drove the lock-in amplifier which in turn directly drove the high-voltage operational amplifier input.

The phase of the reflected intensity response was compared with the phase of the reference frequency by the lock-in amplifier. Its output voltage was changed so that the phase variation of both corresponded to a symmetric oscillation of the specimen with respect to the reflection maximum (mean angle position equals the Bragg angle).

The frequency of the oscillation was adapted to the characteristic time (filter) of the current amplifier. It had to be chosen taking into account pulse statistics and time characteristics of the monochromator stabilization. We obtained a maximum oscillation frequency of 40 Hz. It did not collide with the higher frequency of the monochromator stabilizer. The accuracy of the coarse angle adjustment must prevent a ‘skipping’ from layer to substrate reflection (angle distance 0.11° in 2θ , see Fig. 3).

At every energy step after setting the coarse reflection position $\theta(E)$ of the specimen, a time delay of 4 s was

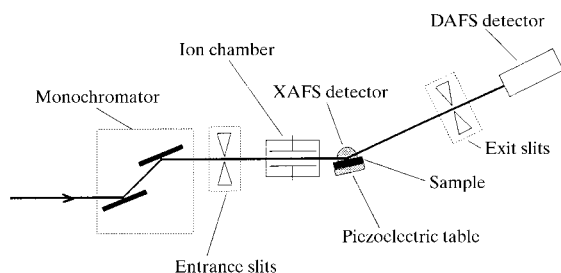


Figure 2
Set-up of DAFS experiments used at HASYLAB (BW1).

sufficient for piezoelectric fine adjustment before starting measurement of the DAFS reflection intensity.

DAFS experiments using (Ga,In)P 333 and $\bar{3}33$ reflections were carried out in the energy range 10300–10900 eV with an energy step width of 3 eV and a measuring time of 10 s per step. Fig. 4 shows the measured DAFS reflection intensities of the (Ga,In)P 333 and $\bar{3}33$ reflections. Simultaneously to the DAFS reflection intensity, the Ga *K*-fluorescence radiation was recorded (reduction angle of about 3°) setting the detector in front of the specimen surface. The total absorption coefficient of the (Ga,In)P layer was determined for the absorption correction making use of the Ga-*K* XAFS signal.

3. DAFS signal analysis

The DAFS intensity for a Friedel pair of reflections $hkl/\bar{h}\bar{k}\bar{l}$ was analyzed. The general approach follows that given by Sorensen *et al.* (1994). While these authors restricted themselves to the analysis of a 004 reflection (which is independent of inversion symmetry), we will derive in detail the more general case of reflections sensitive to inversion symmetry and compare our experimental results with these predictions.

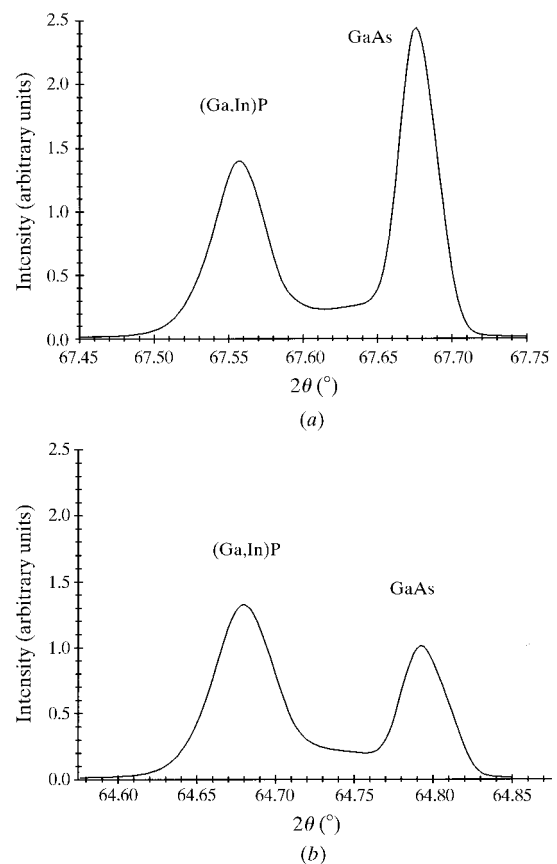


Figure 3
Diffraction pattern in the range of the (Ga,In)P 333 and GaAs 333 reflections at a photon energy of (a) 10200 eV and (b) 10600 eV.

Compared with XAFS analysis, the procedure of separating DAFS from the measured intensity $I(E)$ of a Bragg reflection as a function of energy E has some peculiarities:

(i) The reflected intensity has superimposed on it the XAFS signal averaged over all the anomalous scatterers in the specimen, which requires a thorough absorption correction.

(ii) In the case of non-centrosymmetric single crystals, the DAFS of the participating anomalous scatterers depends on the scattering phase. This means a correct orientation of the crystal is a prerequisite for DAFS analysis. Otherwise different short-range-order parameters will be obtained for one and the same atom depending on the sign of the reflection used.

Referring to the first item, we have used the measured fluorescence intensity of the anomalous scatterer to gain the absorption correction from the total absorption coefficient. This procedure has already been described by Meyer *et al.* (1995) for another system. To eliminate the influence of the individual reflection plane (phase) on DAFS, the measured reflection intensities $I_{M \text{ DAFS}}$ (Fig. 4) had been normalized with the aid of calculated smooth intensities [calculated for kinematic reflection (layer thickness of the order of $1 \mu\text{m}$)] as a function of the scattering phase angle.

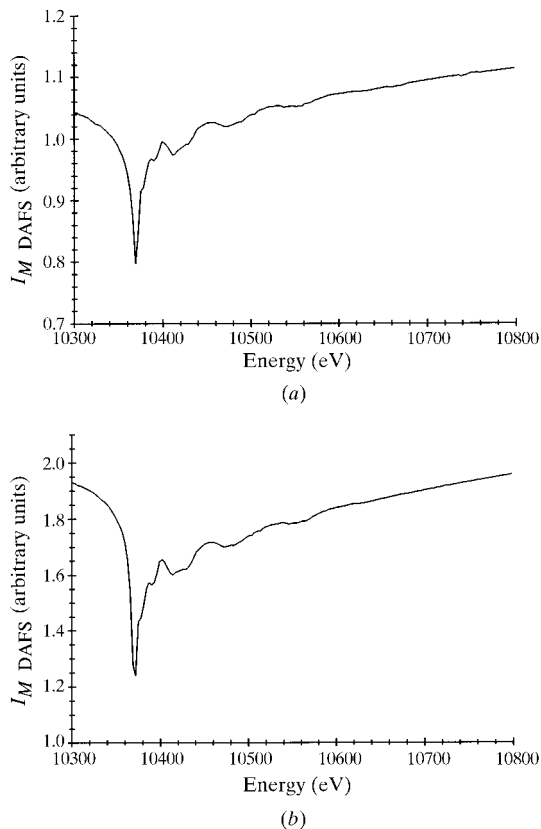


Figure 4
DAFS reflection intensities *versus* energy for (a) the (Ga,In)P 333 reflection and (b) the (Ga,In)P $\bar{3}33$ reflection.

As a result of the absorption correction and normalization, we obtained the DAFS spectra shown in Fig. 5 (complete structure factor F). For normalization, the measured intensities were divided by adapted regression functions [polynomials of the degree of about 20, resonant atomic scattering amplitudes calculated on the basis of Cromer & Liberman (1970)]. As these regression functions turned out to be almost linear functions with a slope near zero, it followed that the instrument function for this energy range is represented by a smooth monotonic function. Within this procedure the other usual corrections of diffractometry, such as polarization correction, have also been carried out.

As an example of DAFS data analysis the GaP 333 and $\bar{3}33$ reflection intensities of the zinc-blende-type structure [space group $F\bar{4}3m$ (216)] will be described, *i.e.* where Friedel's law breaks down (Coster *et al.*, 1930).

The structure factor A_0 (smooth run disregarding contributions of fine structure) for the 333 reflection (Ga atoms on Zn sites and P atoms on S sites) with non-resonant atomic scattering amplitudes $f_{0\text{Ga}}$ and $f_{0\text{P}}$ and their resonant (anomalous) parts $f'_{\text{sGa}} + if''_{\text{sGa}}$ and $f'_{\text{sP}} + if''_{\text{sP}}$

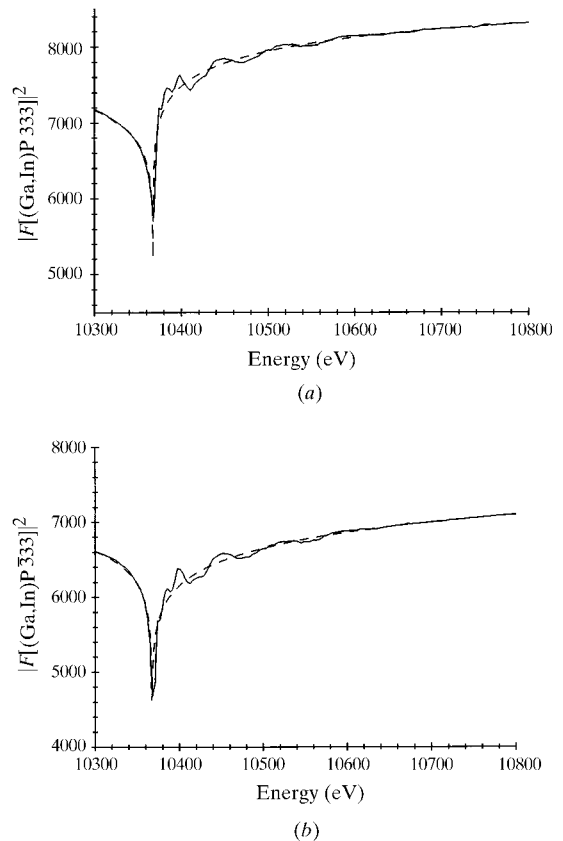


Figure 5
DAFS reflection intensities of the specimen (line) and curves of $|A_0|^2$ (dashed) corrected with respect to the absorption of the radiation on its path through the (Ga,In)P layer and normalized with respect to the theoretical intensities. (a) (Ga,In)P 333 reflection. (b) (Ga,In)P $\bar{3}33$ reflection.

(resulting in corrections of the smooth curve without contributions of fine structure) is given by

$$A_0 = 4(f_{0\text{Ga}} + f'_{s\text{Ga}} + if''_{s\text{Ga}}) + i4(f_{0\text{P}} + f'_{s\text{P}} + if''_{s\text{P}}), \quad (1)$$

where the real part $\text{Re}(A_0)$ and the imaginary part $\text{Im}(A_0)$ can be combined to

$$\text{Re}(A_0) = 4(f_{0\text{Ga}} + f'_{s\text{Ga}} - f''_{s\text{P}}) \quad (2)$$

and

$$\text{Im}(A_0) = 4(f''_{s\text{Ga}} + f_{0\text{P}} + f'_{s\text{P}}). \quad (3)$$

Thus for this reflection the intensity I is represented by

$$I \simeq |A_0|^2 = 16[(f_{0\text{Ga}} + f'_{s\text{Ga}} - f''_{s\text{P}})^2 + (f''_{s\text{Ga}} + f_{0\text{P}} + f'_{s\text{P}})^2]. \quad (4)$$

Analogously, the intensity I of the $\bar{3}33$ reflection is obtained as

$$I \simeq |A_0|^2 = 16[(f_{0\text{Ga}} + f'_{s\text{Ga}} + f''_{s\text{P}})^2 + (f''_{s\text{Ga}} - f_{0\text{P}} - f'_{s\text{P}})^2]. \quad (5)$$

Fig. 6 shows the oscillating portions of the reflection intensities (differences of the full and dashed curves in Fig. 5, filtered with respect to high-frequency noise). F_{os} stands for the oscillating part of the complete structure factor (F). The pronounced oscillation of the DAFS signal compared with the calculated smooth reflection intensity

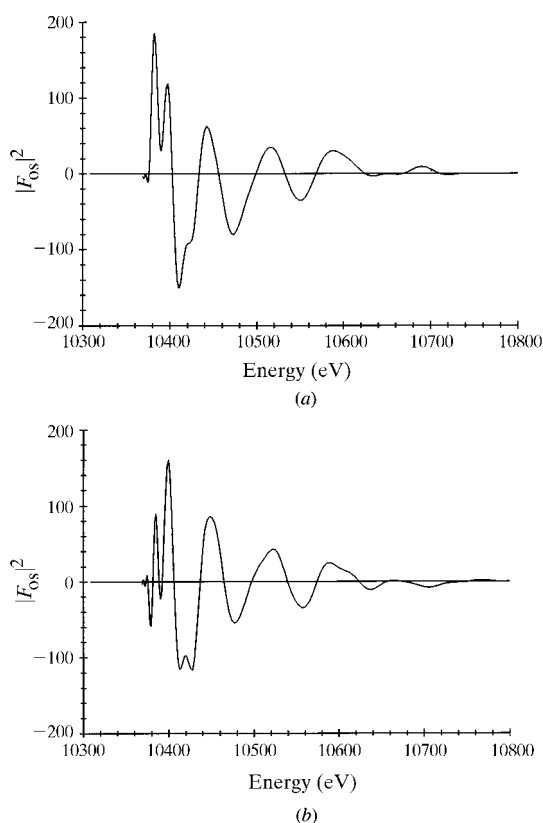


Figure 6
Oscillating contributions of the DAFS reflection intensities. (a) (Ga,In)P 333 reflection. (b) (Ga,In)P $\bar{3}33$ reflection.

encouraged further analysis steps. Note that recognizable differences result from different weighting of the contributions of the real or imaginary parts of the complex-valued fine-structure function to the oscillating part of the reflection intensities. This will be discussed in detail now.

Evaluation of the complex-valued fine-structure function from the oscillating contributions of intensities was described by Sorensen *et al.* (1994). To simplify the representation, the corresponding equations for GaP will be given here. Equations for (Ga,In)P may be obtained by substituting half of the Ga atoms by In atoms, considering the fact that, for the experiment at the Ga- K absorption edge, In does not occur as the predominant anomalous scatterer.

Taking into account the oscillating microstructure terms of the atomic scattering amplitudes f'_{osGa} and f''_{osGa} of Ga as a resonantly scattering atom, the complete structure factor F can be written as

$$F = A_0 + 4(f'_{\text{osGa}} + if''_{\text{osGa}}). \quad (6)$$

In accordance with Sorensen *et al.* (1994) the complex-valued fine-structure function $\chi = \chi' + i\chi''$ is connected to the oscillating terms of the atomic scattering amplitudes by

$$f'_{\text{osGa}} = f''_{s\text{Ga}}\chi' \quad \text{and} \quad f''_{\text{osGa}} = f'_{s\text{Ga}}\chi''. \quad (7)$$

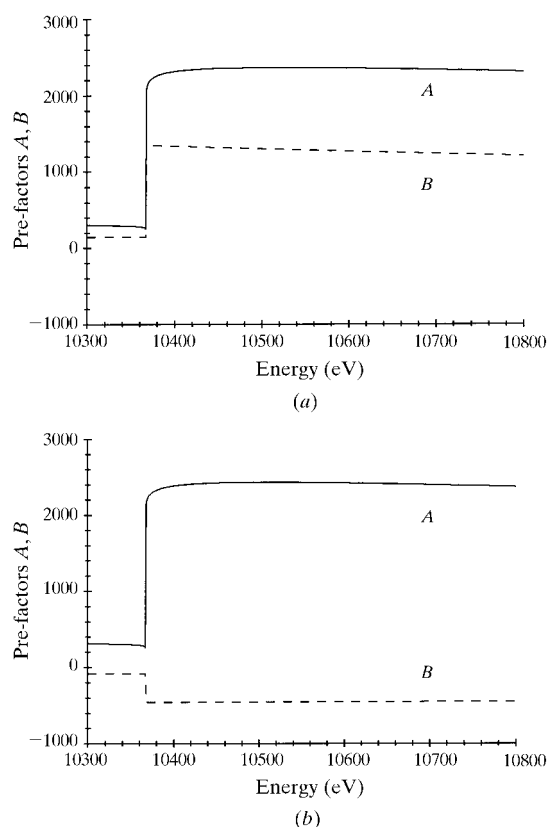


Figure 7
Pre-factors of the contributions of the real and imaginary parts of the complex-valued fine-structure function to the oscillating portions of the measured intensity. (a) (Ga,In)P 333 reflection. (b) (Ga,In)P $\bar{3}33$ reflection.

Neglecting the square terms in f'_{osGa} and f''_{osGa} the intensity becomes

$$I \simeq |A_0|^2 + 2\text{Re}(A_0)4f'_{\text{osGa}} + 2\text{Im}(A_0)4f''_{\text{osGa}}, \quad (8)$$

or, introducing χ ,

$$I \simeq |A_0|^2 + 2\text{Re}(A_0)4f'_{\text{sGa}}\chi' + 2\text{Im}(A_0)4f''_{\text{sGa}}\chi''. \quad (9)$$

Thus, for the GaP 333 reflection we obtain

$$I \simeq |A_0|^2 + 32[(f_{0\text{Ga}} + f'_{\text{sGa}} - f''_{\text{sP}})(f'_{\text{osGa}}) + (f''_{\text{sGa}} + f_{0\text{P}} + f'_{\text{sP}})(f''_{\text{osGa}})] \quad (10)$$

or

$$I \simeq |A_0|^2 + 32f''_{\text{sGa}}[(f_{0\text{Ga}} + f'_{\text{sGa}} - f''_{\text{sP}})(\chi') + (f''_{\text{sGa}} + f_{0\text{P}} + f'_{\text{sP}})(\chi'')]. \quad (11)$$

By taking into account the oscillating terms of the GaP $\bar{3}33$ reflection with Ga as anomalous scatterer, we find

$$I \simeq |A_0|^2 + 32[(f_{0\text{Ga}} + f'_{\text{sGa}} + f''_{\text{sP}})(f'_{\text{osGa}}) + (f''_{\text{sGa}} - f_{0\text{P}} - f'_{\text{sP}})(f''_{\text{osGa}})] \quad (12)$$

or

$$I \simeq |A_0|^2 + 32f''_{\text{sGa}}[(f_{0\text{Ga}} + f'_{\text{sGa}} + f''_{\text{sP}})(\chi') + (f''_{\text{sGa}} - f_{0\text{P}} - f'_{\text{sP}})(\chi'')]. \quad (13)$$

Comparison of these expressions for the different lattice-plane families shows that the different real or imaginary parts of the corresponding structure factors result in different contributions of the real and imaginary parts of χ to the oscillating contributions of the measured intensity.

To illustrate these influences, we write (11) and (13) as

$$I - |A_0|^2 = A\chi' + B\chi'', \quad (14)$$

where pre-factors A and B depend on atomic scattering amplitudes. Fig. 7 shows the pre-factors calculated according to (14) and referred to (11) and (13).

For energies higher than the absorption edge, the contribution of χ' to the oscillating portions of the measured intensity prevails as compared with χ'' for both lattice-plane families. Note that χ'' contributes to the oscillating parts of the measured intensities of the (Ga,In)P 333 and $\bar{3}33$ reflections with opposite sign. At the beginning of the iterative Kramers–Kronig algorithm for calculation of χ' and χ'' , a first approximation for χ' was obtained by dividing the fine structure of the measured intensity by the curve of the pre-factor A , neglecting the influence of χ'' . Then, χ'' was obtained by the Kramers–Kronig transformation of χ' (energy interval 10367–10800 eV). As the magnitude of the pre-factor of χ'' in the case of the (Ga,In)P 333 reflection compared with that of the (Ga,In)P $\bar{3}33$ reflection is greater by a factor of about 3, three iteration steps were necessary in the case of the (Ga,In)P 333 reflection compared with only two iteration steps in the case of (Ga,In)P $\bar{3}33$.

After these iteration steps, no further changes of the solutions for χ' and χ'' occurred within the limits of measurement statistics. In Fig. 8(a) the real part of χ' for

(Ga,In)P (111) planes of the specimen is represented, whereas Fig. 8(b) shows χ'' which was obtained from an iterative Kramers–Kronig algorithm. As a result we find that χ'' is almost equal for both reflections [(Ga,In)P 333 and $\bar{3}33$] and is comparable with the function χ_{μ} , derived from the Ga K -fluorescence XAFS signal.

4. Conclusions

DAFS measurements applied to almost perfect crystals need a precise adjustment of Bragg peak *versus* energy. A programmed coarse adjustment of the sample goniometer combined with a piezoelectric fine adjustment of the specimen proved successful while using the reflected X-ray intensity as feedback signal. DAFS analysis requires a thorough absorption correction, which can be accomplished by measurement of fluorescence intensity of the anomalous scatterer. It has been shown that, similar to single-crystal structure analysis, the lack of inversion

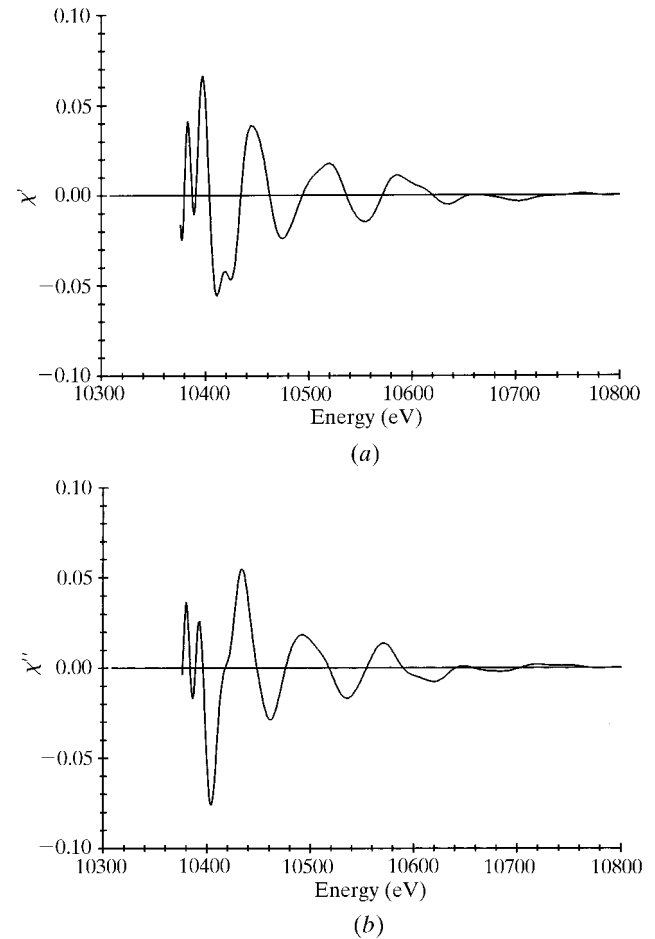


Figure 8

(a) Real part of the complex-valued fine-structure function χ' for the (Ga,In)P (111) planes of the specimen. (b) Imaginary part of the complex-valued fine-structure function χ'' for the (Ga,In)P (111) planes of the specimen.

symmetry has a significant impact upon the DAFS signal, so that DAFS may contribute to structure analysis too.

The authors are indebted to G. Materlik (HASYLAB) for discussions concerning the experimental set-up. They express their gratitude to V. Gottschalch (Leipzig University) for supplying the sample. Financial support by the BMBF, Germany (project No. 05647 ODA 3), is gratefully acknowledged.

References

- Arcon, I., Kodre, A., Glavic, D. & Hribar, M. (1987). *J. Phys. (Paris) Colloq.* **48**(C9), 1105–1108.
- Arndt, U. W., Greenough, T. J., Helliwell, J. R., Howard, J. A. K., Rule, S. A. & Thompson, A. W. (1982). *Nature (London)*, **298**, 835–838.
- Coster, D., Knol, K. S. & Prins, J. A. (1930). *Z. Phys.* **63**, 345–369.
- Cromer, D. T. & Liberman, D. (1970). *J. Chem. Phys.* **53**, 1891–1898.
- Hodeau, J. L., Vacinova, J., Wolfers, P., Garreau, Y., Fontaine, A., Hagelstein, M., Elkaim, E., Lauriat, J. P., Collomb, A. & Muller, J. (1995). *Nucl. Instrum. Methods Phys. Res. B*, **97**, 115–118.
- Lee, P. L., Beno, M. A., Knapp, G. S. & Jennings, G. (1994). *Rev. Sci. Instrum.* **65**, 2206–2209.
- Meyer, D. C., Holz, Th., Krawietz, R., Richter, K., Wehner, B. & Paufler, P. (1995). *Phys. Status Solidi A*, **150**, 603–612.
- Meyer, D. C., Richter, K., Paufler, P. & Krane, H.-G. (1994). *Cryst. Res. Technol.* **29**, K66–70.
- Meyer, D. C., Richter, K., Seidel, A., Schulze, K.-D., Sprungk, R. & Paufler, P. (1995). *HASYLAB Annual Report 1995*, pp. 273–274. HASYLAB, D-22603 Hamburg, Germany.
- Meyer, D. C., Wagner, G., Richter, K. & Paufler, P. (1998). *Phys. Rev. B*. Submitted.
- Mizuki, J. (1996). *X-ray Absorption Fine Structure for Catalysts and Surfaces*, edited by Y. Iwasaka, pp. 372–382. Singapore: World Scientific.
- Ravel, B., Newville, M., Cross, J. O. & Bouldin, C. E. (1995). *Physica B*, **208/209**, 145–147.
- Renevier, H., Weigelt, J., Andrieu, S., Frahm, R. & Raoux, D. (1995). *Physica B*, **208/209**, 217–219.
- Sorensen, L. B., Cross, J. O., Newville, M., Ravel, B., Rehr, J. J., Stragier, H., Bouldin, C. E. & Woicik, J. C. (1994). *Resonant Anomalous X-ray Scattering*, edited by G. Materlik, C. J. Sparks & K. Fischer, pp. 389–420. Amsterdam: Elsevier.
- Stragier, H., Cross, J. O., Rehr, J. J., Sorensen, L. B., Bouldin, C. E. & Woicik, J. C. (1992). *Phys. Rev. Lett.* **69**, 3064–3067.
- Ueda, O., Takikawa, M., Komeno, J. & Umebu, I. (1987). *Jpn. J. Appl. Phys.* **26**, L1824–L1827.
- Vacinova, J., Hodeau, J. L., Wolfers, P., Elkaim, E., Lauriat, J. P., Bouchet-Fabre, B. & Chamberland, B. L. (1995). *Nucl. Instrum. Methods Phys. Res. B*, **97**, 102–106.